

Effect of the Ambient Temperature on the Start-Up of a Multi-Evaporator Loop Thermosyphon

^aL. Araneo, ^bD. Mangini, ^cM. Mameli, ^dS. Filippeschi, ^eG. Valenti, ^fM. Marengo

^a Politecnico di Milano, Via Lambruschini 4A, Milan, Italy. E-mail: lucio.araneo@polimi.it

^b University of Bergamo, Via Galvani 2, Dalmine, Italy. E-mail: danymangini@msn.com

^c University of Pisa, Largo L. Lazzarino, Pisa, Italy. E-mail: mauro.mameli@ing.unipi.it

^d University of Pisa, Largo L. Lazzarino, Pisa, Italy. E-mail: sauro.filippeschi@den.unipi.it

^e Politecnico di Milano, Via Lambruschini 4A, Milan, Italy. E-mail: gianluca.valenti@polimi.it

^f University of Brighton, Lewes Road, Brighton, U.K.. Email: m.marengo@brighton.ac.uk

1. Introduction

Two-phase heat transfer devices are becoming fairly ubiquitous; the capability to transport heat at high rates over appreciable distances, without any external pumping device, the low cost, durability and relatively simpler modeling/design process, make this technology very attractive for many thermal management applications. Indeed, such devices have been investigated in plenty of fields such as: nuclear plants, energy systems, solar heat recovery, air conditioning, electronic cooling in avionics and in railway traction. As a consequence, they can operate under different environmental conditions that can affect their behavior. Nevertheless, it is difficult to find in literature something related to the effect of the ambient temperature on the thermal performance of such devices. The actual temperature, varying the thermo-fluid properties of the fluid inside the device, the condensation and the evaporation phenomena, could be an important parameter that can affect the performance. In this work a Multi-Evaporator loop thermosyphon is tested at different ambient temperatures, ranging from $-20\text{ }^{\circ}\text{C}$ up to $30\text{ }^{\circ}\text{C}$. The start-up behavior, as well as the thermal performance, are analyzed by means of temperature and pressure measurements and fluid flow visualization.

2. Experimental apparatus

The device consists in an aluminum tube (I.D./O.D. 3/5 mm), bended into a planar serpentine with five U-turns in the heated zone (Fig.1). The tube is closed in a loop, evacuated and partially filled with FC-72, with a filling ratio of 50%. A transparent section (50 mm, axial length), closing the loop at the condenser zone, allows the fluid flow visualization.

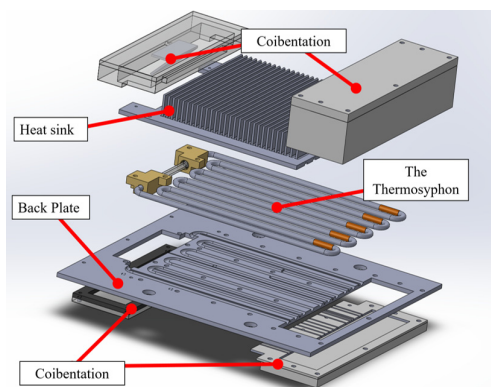


Figure 1: Exploded view of the test section.

A high speed camera (Ximea®, MQ013MG-ON objective:

Cosmicar/Pentax® C2514-M, frame rate up to 200 fps) records the flow motion. Images are post-processed in order to calculate the bubbles speed. Five heating elements are positioned just above the U-turns, providing non symmetrical heating and establishing a two-phase flow circulation, as already demonstrated [1,2]. The condenser section is 165 mm long and it is embedded into a heat sink, which is cooled by means of two air fans (Sunon® PMD1208PMB-A). The temperature evolution recorded both at the condenser and at the evaporator zone by means of 16 T-Type thermocouples allows to calculate the overall thermosyphon thermal performance. A pressure transducer (Kulite®, XCQ-093, 1.7 bar A) records the local pressure (Fig. 2) and it is synchronized via software to the images.

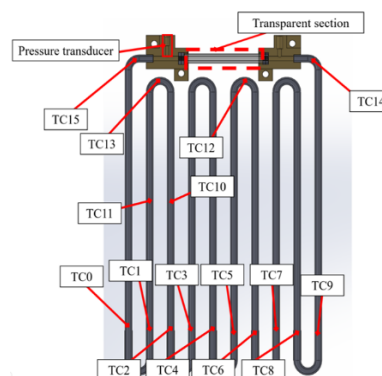


Figure 2: Thermocouples and pressure transducer position along the device.

3. Experimental Procedure

Tests are performed imposing a constant ambient temperature by means of a thermal chamber (Discovery 1200 by Angelatoni Test Technologies®) and changing the global heat power input provided by the device. The ambient temperatures tested are $-20\text{ }^{\circ}\text{C}$, $-10\text{ }^{\circ}\text{C}$, $0\text{ }^{\circ}\text{C}$, $10\text{ }^{\circ}\text{C}$, $20\text{ }^{\circ}\text{C}$ and $30\text{ }^{\circ}\text{C}$. For each ambient temperature tested the heater input power, starting from a global power of 10 W, is firstly increased by steps of 10 W, with finer detail in the lower power region to detect when the start-up occurs. Power is furtherly increased with coarser steps up to 150 W. After that, the heating power is reduced following the same heating steps, in order to understand the role of possible inertial effects on the flow motion de-activation. Then, the power is increased again in order to detect possible hysteresis phenomena with respect to the first start-up. All the heating power levels are kept constant for 15 minutes, in order to reach the steady-state conditions. Tests are performed in vertical position, in Bottom Heated mode.

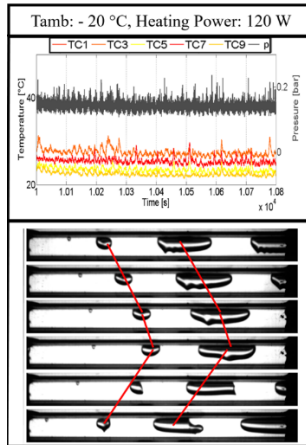


Figure 3. Test with T_{amb} of $-20\text{ }^{\circ}\text{C}$, a) temperatures and pressure; b) Flow oscillations, 50 fps

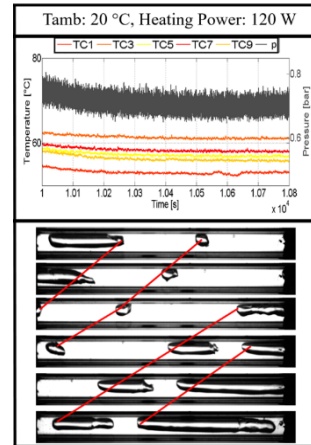


Figure 4. Test with T_{amb} of $+20\text{ }^{\circ}\text{C}$, a) temperatures and pressure; b) Flow circulation, 50 fps.

4. Experimental results

The experimental results show that the ambient temperature clearly affects the device start-up and the internal flow motion. In general, five different thermo-fluid behaviors can be recognized:

- *No motion*: both the evaporator and the condenser do not present any temperature fluctuation; the pressure in the condenser zone is stable at the saturation value of the working fluid; no flow motion is recognizable from the transparent section. During the power-down case, this phase is called “Complete De-Activation”.
- *Start-Up*: temperature oscillations are recognizable at least in one channel.
- *Unstable Behavior*: after the start-up, the temperatures at the evaporator does not stabilize, i.e. an intermittent flow motion occurs.
- *Full Activation*: all the temperatures at the evaporator zone abruptly decrease while the pressure signal exhibits an intense peak. A vigorous two-phase flow motion is recognizable through the transparent section.
- *Circulation*: the fluid flows in a preferential direction.

Results show that the power levels at which the different thermo-fluid behavior occurs depend on the ambient temperature. The images, coupled with the temperature and pressure trends, permit to draw a flow pattern maps for the experimental matrix (Table 1), establishing a relationship between the two-phase flow motion and the device thermal behavior. For the lowest ambient temperature tested, after the start-up, the device has an unstable behavior for a wide range of power levels. Temperatures do not stabilize and partial activations are detectable.

The thermal behavior is different also after the full activation. At $-20\text{ }^{\circ}\text{C}$, the device is affected by frequent short stopovers that do not prevent it from reaching a pseudo steady state (Fig. 3a). Increasing the ambient temperature at $20\text{ }^{\circ}\text{C}$ and heating up the device with the same power, the temperatures remain stable and the pressure in the condenser zone shows always strong fluctuations (Fig. 4a), evidence of a vigorous two-phase flow motion. The flow motion recorded in the transparent section is different too: for the lowest ambient temperature, the flow is oscillating at 120 W (Fig. 3b), while for the $20\text{ }^{\circ}\text{C}$ case a circulation in a preferential direction is observed (Fig. 4b).

	Power-up phase (Q-up)												Power-down phase (Q-down)											
$-20\text{ }^{\circ}\text{C}$	-	-	-	-	-	S	S	S	S	O	C	O	O	O	S	S	S	S	-	-	-	-		
$-10\text{ }^{\circ}\text{C}$	-	-	-	-	-	S	S	S	O	C	C	C	C	C	O	S	S	S	-	-	-	-		
$0\text{ }^{\circ}\text{C}$	-	-	-	-	-	O	O	C	C	C	C	C	C	C	O	S	S	S	-	-	-	-		
$10\text{ }^{\circ}\text{C}$	-	-	-	-	-	O	C	C	C	C	C	C	C	C	C	C	S	S	-	-	-	-		
$20\text{ }^{\circ}\text{C}$	-	-	-	-	-	S	O	C	C	C	C	C	C	C	C	C	C	O	-	-	-	-		
$30\text{ }^{\circ}\text{C}$	-	S	S	S	S	C	C	C	C	C	C	C	C	C	C	C	C	O	S	-	-	-		
$q''[\text{W}/\text{cm}^2]$	1.0	2.1	3.2	4.2	5.3	6.4	7.5	8.6	9.7	12.7	16	12.7	9.7	8.6	7.5	6.4	5.3	4.2	3.2	2.1	1			
P[W]	10	20	30	40	50	60	70	80	90	120	150	120	90	80	70	60	50	40	30	20	10			

Second Power-up phase (Q-up 2)											
-	-	S	S	S	S	S	O	O	-	-	$-20\text{ }^{\circ}\text{C}$
-	-	-	-	-	-	S	S	-	-	-	$-10\text{ }^{\circ}\text{C}$
-	-	S	S	S	O	C	-	-	-	-	$0\text{ }^{\circ}\text{C}$
-	-	-	-	S	C	-	-	-	-	-	$10\text{ }^{\circ}\text{C}$
-	-	-	-	S	C	-	-	-	-	-	$20\text{ }^{\circ}\text{C}$
-	-	S	O	C	-	-	-	-	-	-	$30\text{ }^{\circ}\text{C}$
2.1	3.2	4.2	5.3	6.4	7.5	8.6	9.7	12.7	$q''[\text{W}/\text{cm}^2]$		
20	30	40	50	60	70	80	90	120	P[W]		

LEGEND	
-	Test not performed
-	No fluid motion nor temperature fluctuations
S	Partial start-up
O	Oscillation (after full start-up)
C	Circulation (after full start-up)

Table 1. Flow pattern map for all the configurations. The full activation is highlighted with a red contour.

Noteworthy, all the liquid and vapor properties for FC-72, such as the saturation pressure, density, liquid surface tension, liquid Prandtl, specific heat of the liquid phase changes sharply in the selected temperatures range (Table 2).

Temperature ($^{\circ}\text{C}$)	Pressure (kPa)	Liquid Density (kg/m^3)	Vapor Density (kg/m^3)	Liquid Cp ($\text{kJ}/\text{kg}\cdot\text{K}$)	Liquid Kin. Viscosity (cm^2/s)	Liquid Prandtl	Surf. Tension (mN/m)
-20	2,5383	1780,6	0,41045	0,97231	0,0085508	23,156	15,82
-10	4,8176	1760,9	0,75221	0,98803	0,0070558	19,635	14,809
0	8,6037	1741,3	1,3007	1,0041	0,0058892	16,836	13,812
10	14,572	1721,6	2,1389	1,0206	0,0049698	14,59	12,83
20	23,562	1701,6	3,3681	1,0377	0,0042379	12,773	11,863
30	36,584	1681,1	5,108	1,0553	0,0036495	11,289	10,912

Table 2. FC-72 thermo-fluid properties.

Such differences may have a direct impact on the overall heat exchange. Further experimental data are therefore necessary to better understand the effects of the physical parameters.

References

[1] Mangini D., Marni M., Georgoulas A., Araneo L., Filippeschi S., Marengo M., A pulsating heat pipe for space applications: Ground and microgravity experiments, *Int. J. of Thermal Sciences* 95 (2015) 53-63.

[2] Marni M., Mangini D., Vanoli G.F., Araneo L., Filippeschi S., Marengo M., Multi-Evaporator Closed Loop Thermosyphon, *Proc. of 7th European-Japanese Two-Phase Flow Meeting*, Zermatt, Switzerland (2015).